NASA Technical Memorandum 107167

Replication of the Apparent Excess Heat Effect in a Light Water—Potassium Carbonate—Nickel Electrolytic Cell

Janis M. Niedra
NYMA, Inc.
Cleveland, Ohio

Ira T. Myers, Gustave C. Fralick,
and Richard S. Baldwin
Lewis Research Center
Cleveland, Ohio

February 1996

National Aeronautics and
Space Administration

NASA Technical Memorandum 107167

REPLICATION OF THE APPARENT EXCESS HEAT EFFECT IN A LIGHT WATER-POTASSIUM CARBONATE-NICKEL ELECTROLYTIC CELL

Janis M. Niedra
NYMA, Inc.
Cleveland, Ohio

Ira T. Myers, Gustave C. Fralick, and Richard S. Baldwin
Lewis Research Center
Cleveland, Ohio

February 1996
National Aeronautics and Space Administration

ABSTRACT

Replication of experiments claiming to demonstrate excess heat production in light water-Ni-K_2CO_3 electrolytic cells was found to produce an apparent excess heat of 11 W maximum, for 60 W electrical power into the cell. Power gains ranged from 1.06 to 1.68. The cell was operated at four different dc current levels plus one pulsed current run at 1 Hz, 10% duty cycle. The 28 liter cell used in these verification tests was on loan from a private corporation whose own tests with similar cells are documented to produce 50 W steady excess heat for a continuous period exceeding hundreds of days. The apparent excess heat can not be readily explained either in terms of nonlinearity of the cell's thermal conductance at a low temperature differential or by thermoelectric heat pumping. However, the present data do admit efficient recombination of dissolved hydrogen-oxygen as an ordinary explanation. Calorimetry methods and heat balance calculations for the verification tests are described. Considering the large magnitude of benefit if this effect is found to be a genuine new energy source, a more thorough investigation of evolved heat in the nickel-hydrogen system in both electrolytic and gaseous loading cells remains warranted.

BACKGROUND

Motivated by the possibility of a new and practical source of abundant energy, a growing flurry of activity continues around the world to replicate, control and understand the source of anomalous heat in the so-called 'cold fusion' effect, first reported in March, 1989 by Fleischman, Pons and Hawkins [1] and also by Jones et al. [2] in electrochemical cells that load deuterium into metallic palladium or titanium. The initial disappointment at lack of experimental reproducibility has by now been compensated to a fair degree by the realization that special and usually difficult to achieve conditions [3] are necessary before the Pons-Fleischman effect can be observed. For example, it is now known that a high D/Pd loading ratio is one such difficult necessary condition and that likely there are others. Thus in the EPRI program [4] on deuterated metals, McKubre et al. report [5] that in a batch of Pons-Fleischman type cells, carefully prepared for precision

calorimetry, every cell achieving a D/Pd>0.95 showed excess heat, whereas none did that had a D/Pd<0.90. This and other effects, such as the frequently long time delay to onset of excess heat, were not fully appreciated at the time of the initial high profile, negative follow-up reports from Harwell [6], Caltech [7, 8] and M.I.T. [9]; moreover some of this work was done in haste and under great pressure of public scrutiny. These early follow-up reports may now be mostly of historical interest, as controversy regarding their calorimetric [10] and data reduction [11] methods has been raised.

Modern cells of various types have been reported to produce 50 W or more of excess power for hundreds of days, to have power multiplication factors over 10, and to achieve specific powers as high as ~4 kW/cm^3 [12]. If true, such data clearly exclude by orders of magnitude an and ordinary chemical explanation and force one to consider various lattice assisted nuclear channels, or exotic quantum chemistry (electron transitions catalyzed to unusual, deep atomic levels [13, 14, 15, 16] and also the subsequent fusing of the "shrunken" atoms), and the even more exotic possibility that somehow space energy, such as effects of the electromagnetic zero-point fluctuations, is involved.

It seems fair to say, however, that many still doubt the quality of evidence for the existence of consistent anomalous heat, citing the sporadic reproducibility and paucity of compelling evidence, nevertheless, current experimental emphasis is shifting away from mere replication of the basic effect to developing it in diverse embodiments such as cells based on gas phase interactions with certain metals, light water-K_2CO_3-Ni, molten salt electrolytes, proton conductors , etc. such alternatives may offer specific advantages for the generation of power and understanding of the underlying mechanisms. foreign overview of the latest experiments and the diverse contending theories, the reader may peruse the series of proceedings of the nth international conferences on cold fusion (lately ICCF for and ICCF5).

THE LIGHT-WATER CELL TESTED AT NASA

If the anomalous heat effect is found to be genuine, then it may be useful as a power source to replace radioisotope thermal generators for planetary spacecraft or other applications. An opportunity arose in 1994 to obtain, on loan from the Hydro catalysis Power Corporation, a light water cell for verification testing. the relative simplicity and reliability of the light water-Ni-K_2CO_3 electrolytic cell made it particularly attractive for startup experimentation into this anomalous heat effect.

The existence of an excess heat effect in electrolytic cells based on a platinum (coated) anode and a nickel cathode immersed in a light-water solution of K_2CO_3 was first reported by R.L. Mills and S.P. Kneizys [16], although the possibility was stated earlier by S. Pons et al. in a patent application [17]. The effect was soon verified by V.C. Noninski [18] and continues as an active topic of research at numerous laboratories.

Prevailing experience has it that only rarely do the light-water cells using either K_2CO_3 or Rb2CO3 fail to produce at least some apparent excess heat immediately upon electrolysis, although full power may take months to develop. In contrast, cells based on Pd and D2O often remain inactive for many days and require very careful selection and loading of the Pd.

The cell obtained was a rather large sized demonstrator, operating with 28 1 of 0.57 M K_2CO_3 solution in deionized, but otherwise ordinary, water in a 10-gal. polyethylene tank (Nalge 54100-0010). Its anode was a set of 10 platinized 1.6"×10" titanium strips and 5 platinized 1"D×8" titanium tubes. And the cathode consisted of 5000 m of 0.5 mm D cold drawn nickel wire, wound as 150 sections, each 33 m long, on a perforated, 5 gal. polyethylene bucket. The 15 anode sections were suspended in a circular array close to the inner wall of this bucket from a 12¼" D polyethylene disk covering the top of the bucket and located several inches above the liquid level. Cathode and anode connections were brought out from the air space between the disk and the outer lid by means of two ½"Dx4" plated steel carriage bolts. Small holes were available in the outer lid and in the disk for insertion of the rod of a stirring paddle and thermocouples into the volume of the inner bucket. This cell came equipped with a 57.6 Ω, 1000 W, incoloy cased and teflon jacketed heating rod for on-the-fly calorimetric calibration.

Another cell, identical except for a missing anode structure, was obtained to provide a stable ambient temperature reference by averaging the short-term air temperature fluctuations.

The cell tested at NASA is thus nearly the same as the one pictured and described in more detail under "Thermacore Experiment 4" in Reference 15, except that the Thermacore cell used an additional, inner cathode wound from 5000 m of nickel wire.

EXPERIMENTAL SETUP AND PROCEDURES

The two cells, the active one on the left and blank reference on the right, were placed side by side in a hood, as shown in Figure 1, with their centers about 48 cm apart and 33 cm behind the draw window. Both cells sat on top of identical, 1" thick, closed cell, plastic foam pads placed in plastic trays; pad compression over the weeks of operation were minor. During operation, the bottom edge of the hood draw window was kept at a fixed market, level with the tops of the cells. in this way the cells were equally cooled by a steady, 0.7 m/s breeze driven by the hood fan, reducing the vagaries of air convection and variation of cell thermal conductivity with cell temperature. room temperature variations were moderated only by the basement location, as no thermostatic control was available. Although room air temperature variations up to a few degrees C were experienced during some days, their effect appeared to be well canceled by referencing the active cell temperature rise with respect to the thermally matched blank cell. The room temperature instability unfortunately did make it difficult to obtain reliable data of cell thermal conductivity directly with respect to the ambient air and heater power below 50 W. No experiments were performed involving electrolysis action in both cells simultaneously (such as comparing the action of K_2CO_3 and $NaCO_3$ solutions in the two cells up operated in series) because our blank had no anode.

During steady dc electrolysis, all data was recorded on a Yokogawa model HR2300 multichannel strip chart recorder. This instrument can resolve 0.1 °C using type T thermocouples on any channel program for temperature. The actual thermocouple wire used was type T duplex, Teflon covered and of enhanced accuracy, obtained from Omega Engineering, Inc. and labeled as “special limits of error.” With this wire, the 3 thermocouples used to measure the electrolyte temperature near its center, top and bottom were found to track each other within 0.1 °C from room temperature to 72 °C. In all, 5 temperature probes were monitored: air temperature at hood

entrance, active cell electrolyte temperature at three gaps and blank cell water temperature and mid depth. The average of the 3 electrolyte temperatures was computed by the HR2300 and also recorded, as was the difference between this average in the blank cell temperature. All immersed thermocouples were electrically isolated from the electrolyte by 6 mm OD (3.5 mm ID) glass tubing, fused shot at one end.

The dc voltage of interest, i.e. at the cell and heating rod terminals as well as from current shots, were routed to the HR 2300 and recorded individually. Electrolysis current was sensed by a 1 mΩ precision shunt and the dc power heating rod current was sensed by a 66.67 mΩ precision shunt. Power computations were done by multiplication and scaling internal to the HR 2300 and the results were recorded. I checked with a Racal-Dana Series 6000 digital multimeter revealed that the voltage and power values displayed digitally by the HR to 300 were accurate to at least ±0.1%. All the HR 2300 input channels were operated floating differential. Also, the output of the 6 V, 50 A electrolysis power supply, a Kepco model ATE6-50M, was entirely dc isolated. With these precautions the chance of any significant ground loop induced error was minimal.

Since the thermal time constant of the cell in the setup was observed to be 5.5 hours, uncontrolled drift of environmentally sensitive parameters could waste many hours of running time and create errors. Primarily this involves control of the heater and electrolysis powers. In the case of electrolysis power, it seemed best for two reasons to fix the cell current and let the voltage drift with the cell temperature. First, at a normal operating point, the cell differential resistance is low, meaning that the current will be very sensitive to small changes in cell voltage or temperature, making control by voltage difficult. Second, one expects any excess heat to basically depend on the current, because the rate of delivery of hydrogen ions to the nickel surface is proportional to the current.

The heater rod in the active cell was used to develop the curve of temperature rise ΔT, as referenced to the unheated blank cell, versus ohmic power dissipated in the active cell by observing the steady state ΔT at selected heater powers. The slope of this line is just the thermal resistance of the cell and the process of generating such a line during electrolysis is called calibration on-the-fly [15,16] An on-the-fly calibration is necessary, for as will be shown, the effects of electrolysis can significantly affect the cell thermal resistance.

To keep heater power constant, even as the heater resistance or supply voltage varies, we used a precision constant power controller. This was a circuit based on analog multiplication and feedback techniques controlling a series-pass power MOSFET and similar to load controllers described by J.M. Niedra [19]. Using a 100 V dc supply, any preset power up to 120 W and stable to within +0.5% could easily be delivered to the heater.

During the regular runs, the active cell was stirred continuously by means of a small teflon half-moon attached to the end of a glass rod rotating at a constant 250 rpm, but the blank cell was stirred only intermittently to eliminate the 0.5 °C or so temperature stratification that could be seen in the water if left undisturbed for a day. Preliminary experiments with the unheated blank cell had shown that in an undisturbed cell suddenly so stirred, any small temperature nonuniformity returned to within 0.1 °C in a minute or two. Further, even after 27 hours of

stirring at 315 rpm and with the hood fan off, no clear temperature rise above ambient could be resolved (0.1 to 0.2 °C). Hence the paddle arrangement and its 250 rpm speed was judged entirely satisfactory, producing a negligible contribution to the steady ΔT.

Pulse mode control of the electrolysis current has been claimed to increase the ratio of excess heat to input power, both in D_2O-Pd [20] and H2O-Ni cells [15]. We tested this mode, as time permitted, for at least a 1 Hz pulse repetition rate at 10% duty cycle. The above mentioned power supply was found to be a good source of sharply rectangular current pulses, when operated in its voltage programmed current mode, with peak current set by the current limiter. Current-to-voltage conversion was done by a 0.010 Ω shunt, whose performance with pulses was verified by comparison to a high speed current probe. To simultaneously record the rectangular cell current pulses and associated terminal voltage, we used two Tektronix type 11A33 differential comparators in a DSA602A digitizing oscilloscope mainframe. The instantaneous product of cell current and voltage was recorded as well. Also, null input recordings were taken immediately after a data recording in order to correct for dc offsets in the 11A33s, which were observed at times to be as much as several percent of the signal amplitude. Null recording provided the only means of baseline correction for the cell voltage waveform record, because the cell voltage did not decay to zero during the cycle. As a check on the digitized data, time-averaged cell current and voltage, formed by 100 S time constant RC networks, were recorded with the HR2300.

ANALYSIS OF DATA

Blank cell thermal conductance

One expects to observe some differences in the steady state heat loss characteristics, or thermal conductance κ, of the blank cell and the active cell during electrolysis. Additional water vapor being carried away in the evolved H_2 and O_2 gas bubbles may well contribute an extra heat loss during electrolysis. And as the electrolysis current is increased, the evolving gases may conceivably contribute to a decrease in κ due to their insulating effect. The heat loss contribution to κ arising from the specific heats of the H_2 and O_2 seems negligible, however, being only about 2.16×10^{-4} $WA^{-1}°K^{-1}$ I, where I is the electrolysis current. Thus for I=10 A, this additional loss is only a few milliwatts per °K. This heat loss has been estimated using the gas specific heats c_p of 28.7 and 26.0 Joule/(mole °K) for H_2 and O_2, [21] respectively, and assuming 100% Faradaic efficiency. Finally, the welding cables clamped to the electrolysis electrode terminals may have contributed a slight additional, temperature dependent heat loss to the active cell. This effect too seemed to be minor, as the temperature rise of the top of the cell was always much less than that of the liquid contained below. In any case, all heat losses for the active cell are automatically included by the on-the-fly calibration.

A number of heat loss calibration runs were performed with the blank cell, loaded with 28.0 liters of deionized water. This amount of water contributes 1.17×10^5 J/°K to the heat capacity, whereas the 8.75 kg of Ni wire contributes only 3.88×10^3 J/°K, with contributions from the other cell hardware being negligible. At least 24 hours were allotted for the cell to reach equilibrium temperature at each of the heater powers set by the precision controller.

The result of the first 4 blank cell heat loss calibration runs is represented by the lower line in Figure 2, which has a reciprocal slope of κ_{bl}=6.13 W/°K. The 3 lower power points are seen to be very well aligned with the origin, but the 125 W point droops slightly. The reason for this droop was thought to be the onset of more rapid water vaporization at the 43 °C temperature of the 125 W point. Therefore a straight line through the origin was fitted to the 3 lower points only. No points below 50 W were taken because of lack of time and the observation that the ¼ inch thick, plastic underpad used initially had compressed to an unacceptably thin 1/8 inch under the weight of the cell. Thereafter a 1 inch thick plastic foam underpad was substituted, which suffered only minor relative compression. The upper straight line through the origin in Figure 2 represents the new characteristic, again ignoring the 125 W point. Now the reciprocal slope is a slightly lower κ_{bl}=5.85 W/°K, which is the same as the 0.17 °C/W on-the-fly coefficient at I_c=50 A given for the Thermacore experiment no. 4. Unfortunately the 75 W point turned out to be the lowest power data obtained with the thicker pad, because lack of time and an unstable room temperature caused by weather made it impossible to take accurate low power points.

In spite of the lack of lower power calibration points, the good alignment with the origin of the points obtained (except for the highest power ones) is evidence that κ is a constant for ΔT below about 17 °C. The purpose of setting the cells in a vigorously and uniformly flowing airstream was of course to reduce any temperature dependence of κ. As seen below, a highly temperature sensitive κ invalidates, or at least complicates, the usual regressive extrapolation toward the origin in order to find the excess heat.

The presence of additional heat loss channels induced by electrolysis necessitates on-the-fly thermal characterization of the active cell. However, this method has a lower limit on power for a given electrolysis current, because this current dissipates ohmic heat in the electrolyte. Nevertheless, lower ohmic heat points were obtained in some electrolysis runs and these support the constancy of κ with ΔT. The active cell runs also exhibited quite clearly a small, but not insignificant, dependence of κ on the electrolysis current. The blank cell calibration line serves merely as a limiting low current check on the active cell thermal behavior.

Heat balance and the excess heat effect

Figure 3 defines the various input and output powers to the cell viewed as a box enclosing unknown and certainly complex processes. There are only two unquestionably significant power inputs, namely the cell terminal power $P_c=V_c\ I_c$ and the heater power P_h. Note that resistive drops in connections internal to the cell might make the power delivered to the electrolyte slightly less than P_c. Thermoelectric pumping of heat through the electrolysis terminals by the Peltier effect is a consideration that has been drawn as an input power P_{te}. The experimentally negligible Joule heat input P_{st} due to stirring is drawn there also.

The temperature rise dependent heat losses consisting of convection, water vaporization and various conductions are lumped into a thermal loss P_{th} which is just $\kappa\Delta T$ if the process is linear over the ΔT range of interest here. The remaining loss is the energy carried away by the H_2 and O_2 gases escaping the cell. This loss amounts to the energy 4.75×10^{-19} J/molecule of H_2O that could be retrieved if the gases were recombined and condensed to liquid H_2O at the same

temperature. When calculated in terms of I_c, this energy corresponds to the thermoneutral voltage of 1.48 V and the 'gas power' is written as $1.48\ \eta I_c$, where the Faradaic efficiency η may be less than 1 to cover the case of a partial recombination of the H_2 and O_2 within the cell.

The excess heat P_{exc}, if any, is simply the difference between the total output and input powers and can be written as

$$P_{exc} = (P_{th} + 1.48\ \eta\ I_c) - (P_c + P_h + P_{te} + P_{st}). \quad (1)$$

To be useful for computing P_{exc} Eq. 1 must be put into a form that relates closer to what is measured. First we note that the thermal heat loss $P_{th} = P_{th}(I_c, \Delta T)$ is an unknown function, but with the property that $P_{th}\ (I_c, 0)=0$. The simplest such admissible form is $P_{th}=\kappa(I_c)\Delta T$. Informationabout this function must be gleaned experimentally, say by varying Ph with I_c fixed. Pc will then vary also, since the V_c versus I_c characteristic is temperature sensitive. Nevertheless, one can combine some of these variables into a single term

$$P_o \equiv P_c + P_h + P_{te} + P_{st} - 1.48\ \eta\ I_c, \quad (2)$$

representing the part of the total input power that is dissipated as heat in the electrolyte. For a fixed I_c, $P_h=0$ gives the least possible P_o. Even if P_{te} and P_{st} are negligible, the possibility that $\eta<1$ can not be ignored. Therefore it is convenient for plotting purposes to define a 'reduced' dissipated power

$$\tilde{P}_o \equiv P_h + P_c - 1.48\ I_c \quad (3)$$

that underestimates the true dissipation, but is completely determined once P_h and I_c are set. With this definition,

$$P_o = \tilde{P}_o + P_{te} + P_{st} + 1.48\ \eta_{rec}\ I_c, \quad (4)$$

where

$$\eta_{rec} \equiv 1-\eta \quad (5)$$

is a recombination efficiency. With these definitions, Eq. 1 becomes

$$P_{exc} = P_{th} - P_o$$
$$= \tilde{P}_{th} - \tilde{P}_o - (P_{te} + P_{st} + 1.48\ \eta_{rec}\ I_c). \quad (6)$$

One can curve fit experimental data of steady state $(\tilde{P}_o, \Delta T)$, obtained by varying P_h at fixed I_c. This plot can then be extrapolated to $\Delta T=0$ to obtain $\tilde{P}_{o|\Delta T=0}$; the confidence one can place in this extrapolation depends on the scatter of the data, the nature of the fitted curve and the closeness of the data to the origin. As mentioned, $P_{th|\Delta T=0}=0$, regardless of the particular dependence of P_{th} on ΔT. Thus from Eq. 6 and this property of P_{th}, it follows immediately that the true excess heat is

$$P_{exc} = (-\tilde{P}_{o|\Delta T=0}) - (P_{te} + P_{st} + 148\ \eta\ I_c) \quad (7)$$

in agreement with considerations in the literature.

If for fixed I_c the $\tilde{P}_o$ versus ΔT is a straight line, then $\partial\tilde{P}_o/\partial\Delta T$ is a constant and hence taking $\partial/\partial\Delta T$ Eq. 6 shows that $P_{th} \propto \Delta T$; this assumes that the terms P_{exc}, P_{te}, P_{st} and $1.48\eta_{rec}$ are constant with ΔT. Any intrinsic dependence of the heat production mechanism on ΔT or T is not revealed by the extrapolation.

A summary of the steady state ΔT versus $\tilde{P}_o$ data obtained at fixed I_c = 5, 10, 20 and 40 A is presented in Figure 4; this data was obtained by varying P_h, as stated under Eq. 6 above. Straight lines gave excellent least squares fits to the data and their extrapolated $\tilde{P}_o$-axis intercepts are $\tilde{P}_{o|\Delta T=0}$=-7.20. -8.57, -11.4 and -8.41 W, corresponding respectively to the above I_c. If the terms P_{te}, P_{st} and $1.48\eta_{rec}I_c$ are negligible (P_{st} certainly is; see EXPERIMENTAL SETUP AND PROCEDURES), then, according to Eq. 7, these ($-\tilde{P}_{o|\Delta T=0}$) are the positive excess powers corresponding to the above 4 dc I_c; however, the P_{te} and $1.48\eta_{rec}I_c$ contributions will be discussed. In general, we shall call ($-\tilde{P}_{o|\Delta T=0}$) the apparent excess power or heat.

Along with each data line in Figure 4, also the blank cell calibration line is redrawn to provide a comparison of their slopes. This comparison shows that $\kappa(I_c) > \kappa_{bl}$ in all 4 cases and that $\kappa(I_c)$ tends to increase slightly with I_c. A summary of this behavior of $\kappa(I_c)$ is presented as a scatter plot in Figure 5, that also includes the κ_{bl} data point as well as κ from a pulse I_c run plotted at its average current $\bar{I}_c$=3.10 A.

Due to time constraints on laboratory space, the only pulse I_c data taken was with 30 A rectangular pulses at a 10% duty cycle and 1 Hz repetition rate, giving the mentioned average $\bar{I}_c$=3.10 A. Values for the on-the-fly calibration plot were obtained by time averaging Eq. 3, etc.. From the corresponding line fitted in Figure 6, the apparent excess heat is found to be only 2.66 W. And the thermal conductance is seen to be very close to that of the blank cell, as already indicated in Figure 5. A sampling of the I_c, V_c and P_c waveforms recorded at thermal equilibrium and P_h=0 is presented along side to show the cell polarization effect. The time averages $\bar{I}_c$ and $\tilde{P}_c$ noted in Figure 6 include small corrections for baseline offsets in the DSA602A.

Internal recombination and water addition

Reliable data on water loss during electrolysis from cells operating without a recombiner is essential to the correct interpretation of the apparent excess heat, especially in low power cases having $-\tilde{P}_{o|\Delta T=0} < 1.48\ I_c$. In such cases a sufficiently high recombination efficiency η_{rec} can imply that P_{exc}=0, even if P_{te} and P_{st} are negligible, as inspection of Eq. 7 shows.

Unfortunately, the run time allotted to each constant heater power P_h was limited to at most a day or two, which precluded the taking of accurate water loss data in our setup. In efforts to compensate for data inaccuracies, a loss rate was calculated for each selected I_c by adding the loss amounts for all the corresponding runs of fixed Ph and dividing by their total time. This procedure reduces the data scatter at the cost of lumping together temperature dependent evaporation rates. Water loss rates so processed are plotted against I_c in Figure 8 and fitted by a straight line. 100% efficient (η=1) electrolysis would generate the loss rate αI_c, where $\alpha = 9.34\times10^{-5}$ g s^{-1} A^{-1} which too is plotted in Figure 8.

The total water loss rate is the sum of evaporation and electrolysis losses, or

$$\mathscr{L} = \mathscr{L}_{ev} + \eta\ \alpha I_c, \tag{8}$$

where $\mathscr{L}_{ev}$ depends on T_c, and hence on I_c and P_h. However, only the I_c dependence of $\mathscr{L}_{ev}$ will be considered below, because for each I_c the P_h dependence has been 'averaged out' in the data of Figure 8. Evaporation dominates recombination in Figure 8, for the data fact that $\mathscr{L} > \alpha I_c$ is the same as

$$\mathscr{L}_{ev} > \eta_{rec}\ \alpha I_c. \tag{9}$$

Although our data is insufficient to place a hard upper bound on η_{rec} a bound tighter than Eq. 9 can be had by substituting the experimental fit

$$\mathscr{L} = \beta I_c + \mathscr{L}_{ev}(0), \tag{10}$$

where $\beta = 9.03\times10^{-5}\ s^{-1}A^{-1}$ and $\mathscr{L}_{ev}(0) = 3.78\times10^{-4}\ g\ s^{-1}$, into

$$\begin{aligned}\mathscr{L} - \alpha I_c &= \mathscr{L}_{ev} + (\eta-1)\ \alpha I_c \\ &= \mathscr{L}_{ev} - \eta_{rec}\ \alpha I_c\end{aligned} \tag{11}$$

to obtain

$$\eta_{rec}\ \alpha I_c = \mathscr{L}_{ev}(I_c) - \mathscr{L}_{ev}(0) + (\alpha - \beta)\ I_c. \tag{12}$$

This formula is useful, because at the lower I_c of the runs the contribution of the I_c to ohmic heating was small as compared to the upper P_h values over which the water loss data was averaged to obtain the points in Figure 8. Thus $\mathscr{L}_{ev}(I_c)$ can not be much greater than $\mathscr{L}_{ev}(0)$ in the present case.

DISCUSSION

To claim the reality of excess heat in the presence of other comparable heat transfer processes, one must support the validity of the extrapolation to get the apparent excess heat ($\tilde{P}_{o|\Delta T=0}$). Both the blank and active cell thermal conductance data shows that these cells in the environment described are well characterized by a thermal conductance κ that depends slightly on the cell current I_c, but not at all on the temperature rise ΔT, at least for $0 \le \Delta T \le 17°C$. The blank cell runs showed in particular that the lower ΔT versus heater power P_h points are well in line with the origin. This eliminates the possibility that the (ΔT, P_h) locus could curve into (0, 0) from above; multiple curvature inflections seem quite unlikely. Further, the active cell constant I_c runs show in Figures 4 and 6 that the thermal conductance characteristic is very linear down to total ohmic heatings of only a few watts, assuming negligible hydrogen-oxygen recombination. Hence there is good evidence for the validity of the linear extrapolation to $\Delta T=0$ of our data.

Accepting the rationale for the apparent excess heat extrapolated from the on-the-fly thermal data, the burden is shifted to showing that the heat additions P_{te}, P_{st} and $1.48\ \eta_{rec}\ I_c$ can not account for the apparent excess. These heats will be discussed below. Worthy of mention is also the possibility of corrections whose omission leads to an underestimate of the excess heat. Ohmic heat is generated in the wires and connections inside the cell, but above the electrolyte.

This heat is included in P_c even though it is not wholly delivered to the electrolyte. Thus in the cell tested, some warming of the external anode terminal was evident for I_c>20 A, while the external cathode terminal remained at about the cell top temperature. Finally, any unrecognized mechanism of electrochemical energy storage is an error on the conservative side.

The stirring power P_{st} is not a contender in accounting for the observed apparent excess heat, because stirring induced ΔT was at the resolution limit, 0.1 °C, of the recorder. This implies a P_{st} below a watt on the blank cell calibration slope κ=5.85 W/°C.

Handel [22] has recently proposed that the thermoelectric power P_{te} into an electrolytic cell may in some cases account for the claimed excess, mainly citing experiments exhibiting a proportionality between steady I_c and excess power. He justifies the required very high (for pure metals) effective differential Peltier coefficient $\Delta\Pi\approx$400 mV by pointing to cases where the excess heat was observed for only a small fraction of the time. We contend, however, that several circumstances greatly reduce the likelihood of, if not entirely eliminating heat pumping as the cause in our case. First, the apparent excess power at I_c=5 A was a steady 1.44 W/A at essentially room temperature, requiring an effective differential Seebeck coefficient $\Delta S=5.27\times10^{-3}$ V/°K; recall that Π=ST and $P_{te}=I_c\,\Delta\Pi=I_c\,T_a\Delta$ S. This value of ΔS is several times that observed even in semiconductors.

Second, a proportionality of excess power to I_c is not supported by the data plot in Figure 7. In contrast, this plot suggests onset of saturation or even interference with rising I_c. Our last, weaker comment is that in our case the P_{te} into the cell vessel is theoretically zero because the electrolysis electrodes exiting the lid are identical. This reduces the problem to one of heat pumping between the junctions in the air space below the lid and the effectively Pt-Ni junction in the electrolyte below. However, no cooling of the exiting electrodes was ever discerned.

To account for all of the observed excess heat by hydrogen-oxygen recombination within the cell requires a recombination efficiency of quite a high magnitude in our case. This efficiency,

$$\eta_{rec} = -\tilde{P}_{o|\Delta T=0}/(1.48I_c), \qquad 13$$

follows from Eq. 7 by setting P_{exc} to zero and neglecting P_{te} and P_{st}. The plot of this η_{rec} in Figure 9, based on the previously derived values of $-\tilde{P}_{o|\Delta T=0}$ at the selected I_c, shows that in the dc case for I_c below 10 A the η_{rec} exceeds 0.55 and grows rapidly to unity at I_c near 5 A. However, our data does marginally admit such an explanation. First, any recombination heat released in the air space between the electrolyte and the leaky lid, where the most active exposed catalyst was nickel wire connecting to the cathode, could hardly be well transmitted to the liquid below. Hence the recombination would have to be within the electrolyte. Using $\mathscr{L}_{ev}(I_c) \approx \mathscr{L}_{ev}(0)$, as argued below Eq. 12 for low I_c, and the experimental data in Figure 8, the loose upper bound on η_{rec} imposed by Eq. 9 falls somewhat below the plot of Eq. 13 in Figure 9. Presumably Eq. 12 restricts η_{rec} even more. Our sparse water addition data thus seems not to entirely favor the recombination explanation, but fails to be decisive either way for lack of accurate $\mathscr{L}_{ev}$ data.

In a recent paper [23] applicable to water-based electrolytic cells, J.E. Jones et al. point out the well known [24] effectiveness of Ni, Pt and Pd to catalyze the recombination of oxygen and hydrogen.

They present electrolytic cell experiments demonstrating the quenching of apparent excess heat in configurations that inhibit the transport of dissolved oxygen to the cathode and hydrogen to the anode. And they further demonstrate the achievement of when O_2 was bubbled through an operating cell. Accepting these results, our data are then generally consistent with the recombination explanation and the behavior of the apparent excess heat with cell current that it predicts.

The fact that the initial slope of the apparent excess heat versus I_c data shown in Figure 7 is comparable to the slope (1.48 W/A) of the maximum gas power line is as predicted at low current density by the recombination hypothesis; the solution of gas becomes more effective at low evolution rates. Related to this, the few reported dc tests of cells nearly identical to the present one, except for the nickel, also suggest a similar slope, even though they produced up to 50 W [15]. Only the pulse mode, not systematically explored here, seems to have produced significantly more energy per coulomb throughput. Therefore, given an equal area of nickel wire, the indications now are that the metallurgy of the nickel greatly affects the saturation P_{exc} but probably less so the initial slope. In fact, subsequent testing of the present cell by the Hydrocatalysis Power Corp. has verified our observations of its low saturation P_{exc} under the same conditions that produced 50 W excess from cells differing only in the source of the nickel wire. For the cell we examined, evidently there was an unfortunate choice of nickel wire from an untested source.

No conclusions can be drawn here regarding exothermal chemical reactions involving the electrodes, because the run times at each cell current and heater power were usually restricted to the minimum needed to establish thermal equilibrium - about 24 hours. However, no ordinary chemical reactions involving nickel are known that could account for the total excess energy from similar Mills type cells claimed to produce 50 W excess for months. And no report of a chemical or metallurgical change of the nickel cathode is known to us.

SUMMARY AND CONCLUSIONS

The light water-Ni- K_2CO_3 electrolytic cell on loan from the Hydrocatalysis Power Corporation clearly exhibited the phenomenon of apparent excess heat when tested at 4 selected dc currents and one pulse mode current. Data was collected using simple 'on-the-fly' calorimetric calibration in the thermal steady state and was reduced to give the apparent excess heat by extrapolation methods that are accepted practice in the field of anomalous heat cell ('cold fusion') research.

Our main findings regarding cell voltages, currents and powers are summarized in Table I. The apparent power gains ranged from 1.06 to 1.68. The apparent excess power of this particular cell saturated at a rather low 11.4 W, at an electrical input power of 59.6 W, using a cell current of 20 A dc, as compared to about 50 W apparent excess reported by other workers for essentially the same cell. We attribute this shortfall to an unfortunate choice of untested nickel from an alternate source.

The power gain given in Table I and plotted in Figure 10 is based on the apparent excess power ($-Pol\Delta T=0$) and is the most optimistic possible, since gas recombination, stirring power and any thermoelectric heat injection are then neglected (see Eq. 7). The maximum possible gas power

(1.48I) is included as part of the output power. The plot of the gain $(P_{exc.apparent}+P_c)/P_c$ in Figure 10 appears of a form decreasing asymptotically to unity for large I_c, as expected for a saturating $P_{exc,apparent}$.

Although our data admits the existence of an unusual source of heat within the cell, it falls far short of being compelling. To delimit the alternatives, we have examined the following factors considered in the literature as potential ordinary causes of multiwatt level, steady state, apparent excess heat in the present type of cell:

1. Unrecognized nonlinearity in the cell thermal conductivity (κ) at low temperature differential (ΔT), leading to erroneous extrapolation for the excess heat.
2. Injection of heat into the cell by thermoelectric pumping (Seebeck effect).
3. Exothermic chemical reactions involving the nickel cathode.
4. Heat from hydrogen-oxygen recombination within the cell.

And we have come to terms with these possibilities as follows:

1. Nonlinearity in κ is contraindicated by the good alignment of our high power thermal calibration points with a straight line through the origin and also by the linear alignment of our 'on-the-fly' calibration points reaching down below 10 W. This linearity was achieved by forced convective cooling.
2. For thermoelectric heat pumping to account for the apparent excess heat would require differential Seebeck coefficients several times those of even semiconductors. Also, such heat pumping through the lid of our cell is zero in first order because the two exiting electrodes were identical.
3. The apparent energy evolved in the present experiments was inadequate to eliminate chemical reactions - runs too short for the power observed. However, this possibility has been examined and rejected by other workers operating very similar cells at 50 W apparent excess heat for months.
4. Our inadequate water accounting data are at least marginally consistent with the recombination explanation of the source of the apparent excess heat, even though this requires recombination efficiencies exceeding 0.55 at 10 A and rising to near unity at 5 A of cell current (Figure 9). Nevertheless, J.E. Jones et al. [23] have claimed to show that light water cells with nickel and platinum electrodes can indeed achieve such high recombination of dissolved oxygen and hydrogen. Also, our Figure 7 suggests this possibility.

Following the principle of simplest explanation that fits the data on hand, recombination becomes the explanation of choice. But even perfect recombination can not account for all of the apparent excess heat in those Mills cells usually operated in a pulsed current mode and reported to produce a thermal output solidly exceeding the VI power input to the cell. These cases at least leave the door open to more interesting possibilities. Considering the potential value of a new energy source, it seems worth while to restudy the Mills type cell in configurations allowing an accurate account for recombination and water loss.

Insufficient resources prevented us from proceeding with a more careful study of the excess heat effect in cell types adapted to bear on specific questions. For example, certain gaseous loading types, such as the D_2-Pd transient pressurizing experiment [25] at NASA or the H_2-Ni heating experiment [26] at the University of Siena, could avoid the complications of electrolytic cells, while exploring possibilities of high temperature operation and radiation emission [27].

ACKNOWLEDGMENTS

The authors gratefully acknowledge both the loan of equipment and technical assistance from the Hydrocatalysis Power Corporation and the support for this work from the Directors Discretionary Fund of the NASA Lewis Research Center.

REFERENCES

[1] M. Fleischmann, S. Pons and M. Hawkins, "Electrochemically Induced Nuclear Fusion of Deuterium", J. Electroanalytical Chem. 261, 1989, pp. 301 - 308.

[2] S.E. Jones et al., Observation of Cold Nuclear Fusion in Condensed Matter", Nature 338, 1989, p. 737.

[3] Cravens, "Factors Affecting the Success Rate of Heat Generation in CF Cells", Proc. of ICCF4, Vol. 2, Maui, Hawaii, December 6-9, 1993, pp. 18-1 to 18-14.

[4] T.O. Passell, "Overview and Status of the EPRI Program on Deuterated Metals", ASME Joint International Power Conference, Phoenix, Arizona, October 2-6, 1994.

[5] M. McKubre et al., "Nuclear Processes in Deuterated Metals", EPRI Report TR-104195, August 1994. See also M. McKubre et al., "Loading, Calorimetric and Nuclear Investigation of the D/Pd System", Proc. of ICCF4, Vol. 1, Maui, Hawaii, December 6-9, 1993, pp. 5-1 to 5-28.

[6] D.E. Williams et al., "Upper Bounds on 'Cold Fusion' in Electrolysis Cells", Nature 342, 1989, p. 375. 7. N.S. Lewis et al., "Searches for Low Temperature Nuclear Fusion of Deuterium in Palladium", Nature 340, 1989, p. 525.

[7] N.S. Lewis et al., "Searches for Low Temperature Nuclear Fusion of Deuterium in Palladium", Nature 340, 1989, p. 525.

[8] G.M. Miskelly et al., "Analysis of the Published Calorimetric Evidence for Electrochemical Fusion of Deuterium in Palladium", Science 246, 1989, p. 793.

[9] D. Albagli et al., "Measurement and Analysis of Neutron and Gamma-Ray Emission Rates, Other Fusion Products, and Power in Electrochemical Cells Having Pd Cathodes", J. Fusion Energy 9, 1990, p. 133.

[10] M.H. Miles et al., "Calorimetric Principles and Problems in Measurement of Excess Power during Pd-D2O Electrolysis", J. Phys. Chem. 98, no. 7, 1994, pp. 1948-1952.

[11] M.R. Swartz, "Some Lessons from Optical Examination of the PFC Phase-II Calorimetric Curves", Proc. of ICCF4, Vol. 2, Maui, Hawaii, December 6-9, 1993, pp. 19-1 to 19-14

[12] M. Fleischmann and S. Pons, "Calorimetry of the Pd-D2O system: from simplicity via complications to simplicity", Phys. Lett. A 176, 1993, p. 118.

[13] J.A. Maly and J. Vavra, "Electron Transitions on Deep Dirac Levels I", Fusion Technology 24, November 1993, pp. 307 - 318.

[14] J.-P. Vigier, "New Hydrogen (Deuterium) Bohr Orbits in Quantum Chemistry and "Cold Fusion" Processes", Proc. of ICCF4, Vol. 4, Maui, Hawaii, December 6-9, 1993, pp. 7-1 to 7-25.

[15] R.L. Mills, W.R. Good and R.M. Shaubach, "Dihydrino Molecule Identification", Fusion Technology 25, January 1994, pp. 103 - 119.

[16] R.L. Mills and S.P. Kneizys, "Excess Heat Production by the Electrolysis of an Aqueous Potassium Carbonate Electrolyte and the Implications for Cold Fusion", Fusion Technology 20, August 1991, pp. 65-81.

[17] S. Pons, M. Fleischmann, C. Walling and J. Simons, "Method and Apparatus for Power Generation," International application published under Paten Cooperation Treaty (PCT/US90/01328; International Publication No. WO90/10935), 13 March 1989.

[18] V.C. Noninski, "Excess Heat During the Electrolysis of a Light Water Solution of K_2CO_3 With a Nickel Cathode", Fusion Technology 21, March 1992, pp. 163-167.

[19] J.M. Niedra, "Analog Synthesized Fast-Variable Linear Load," Proc. of the 26th IECEC, Boston, Massachusetts, August 1991. Also NASA CR-187155.

[20] A. Takahashi et al., "Windows of Cold Nuclear Fusion and Pulsed Electrolysis Experiments", Fusion Technology 19, 1991, pp. 380-390.

[21] CRC Handbook of Chemistry and Physics, 69th Edition, CRC Press, Boca Raton, 1988-1989, p. D-44.

[22] P.H. Handel, "Subtraction of a New Thermo- Electrochemical Effect from the Excess Heat, and the Emerging Avenues to Cold Fusion", Proc. of ICCF4, Vol. 2, Maui, Hawaii, December 6-9, 1993, pp. 7-1 to 7-8.

[23] J.E. Jones et al., "Faradaic Efficiencies Less Than 100% During Electrolysis of Water Can Account for Reports of Excess Heat in "Cold Fusion" Cells", J. Phys. Chem. 99, no. 18, 1995, pp. 6973-6979.

[24] A. McDougall, Fuel Cells, Energy Alternatives Series, John Wiley, New York, 1976, p. 54.

[25] S. Focardi, R. Habel and F. Piantelli, "Anomalous Heat Production in Ni-H Systems," Il Nuovo Cimento 107A, N.1, January 1994, pp. 163-167.

[26] S. Focardi, R. Habel and F. Piantelli, "Anomalous Heat Production in Ni-H Systems," Il Nuovo Cimento 107A, N.1, January 1994, pp. 163-167.

[27] C. Manduchi et al., "Anomalous Effects During the Interaction of Subatmospheric D2 (H2) with Pd from 900 °C to Room Temperature," Il Nuovo Cimento 107A, N.2, February 1994, pp. 171-183.

Table I. Operating characteristics of Hydrocatalysis Power Corporation's demonstration light water-Ni- K_2CO_3 electrolytic cell.

I_c (A)	V_c (V)	Duty Cycle (%)	$V_c I_c$ (W)	P_{exc}, apparent (W)	Apparent Power Gain[3]
5.0	2.12	100	10.6	7.20	1.68
10.0	2.55	100	25.5	8.57	1.34
20.0	2.98	100	59.5	11.4	1.19
40.0	3.36	100	134.5	8.41	1.06
31.0[1]	1.72[2]	10	8.58[2]	2.66	1.31

(1) Peak current of rectangular pulse

(2) Time average

(3) Apparent Power Gain $\equiv (P_{exc,apparent} + V_c I_c) / (V_c I_c)$

Note: usual test duration was about 24 hours at each fixed I_c and heater power

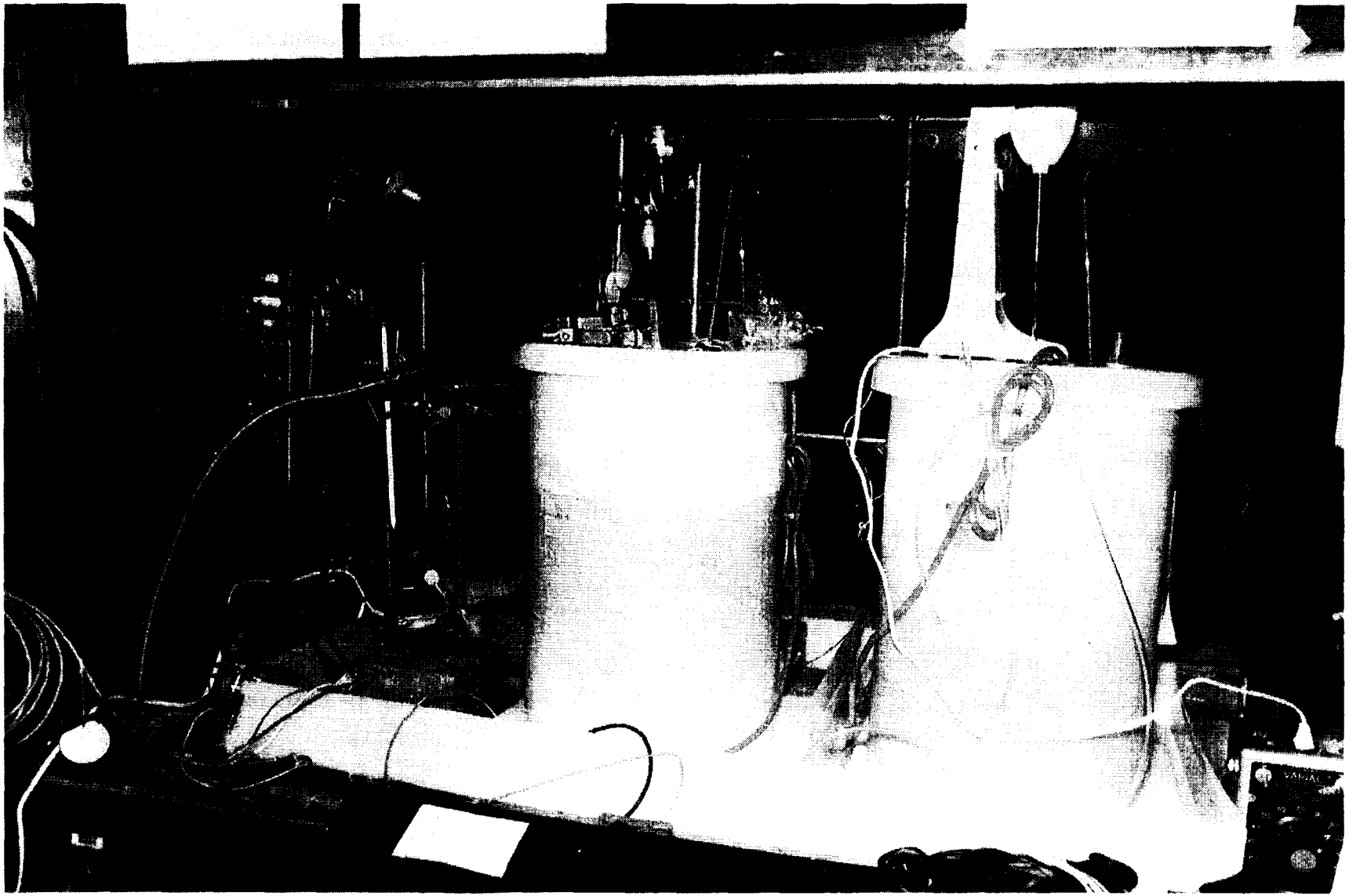

Figure 1. Active (left) and reference cells on the floor of a hood. During operation, the lower sash of the draw window was kept at a height even with the tops of the cells, giving a window airflow of 0.7 m/s.

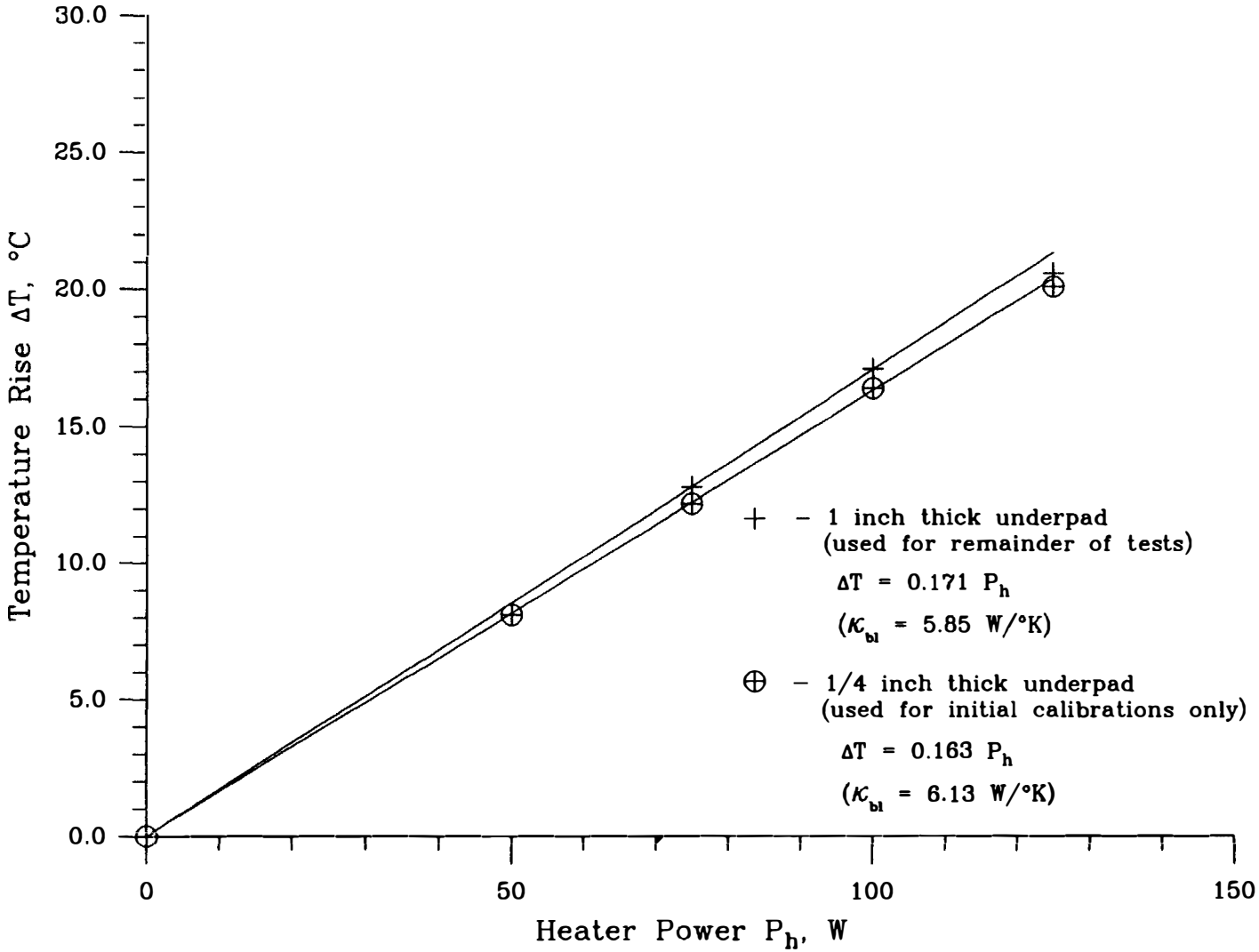

Figure 2. Temperature rise above ambient air (~23 °C) of the blank cell at selected heater powers. Fits are least squares straight lines through the origin, ignoring the 125 W points, which appeared to be drooping due to the increased water vaporization at their temperature (~43 °C).

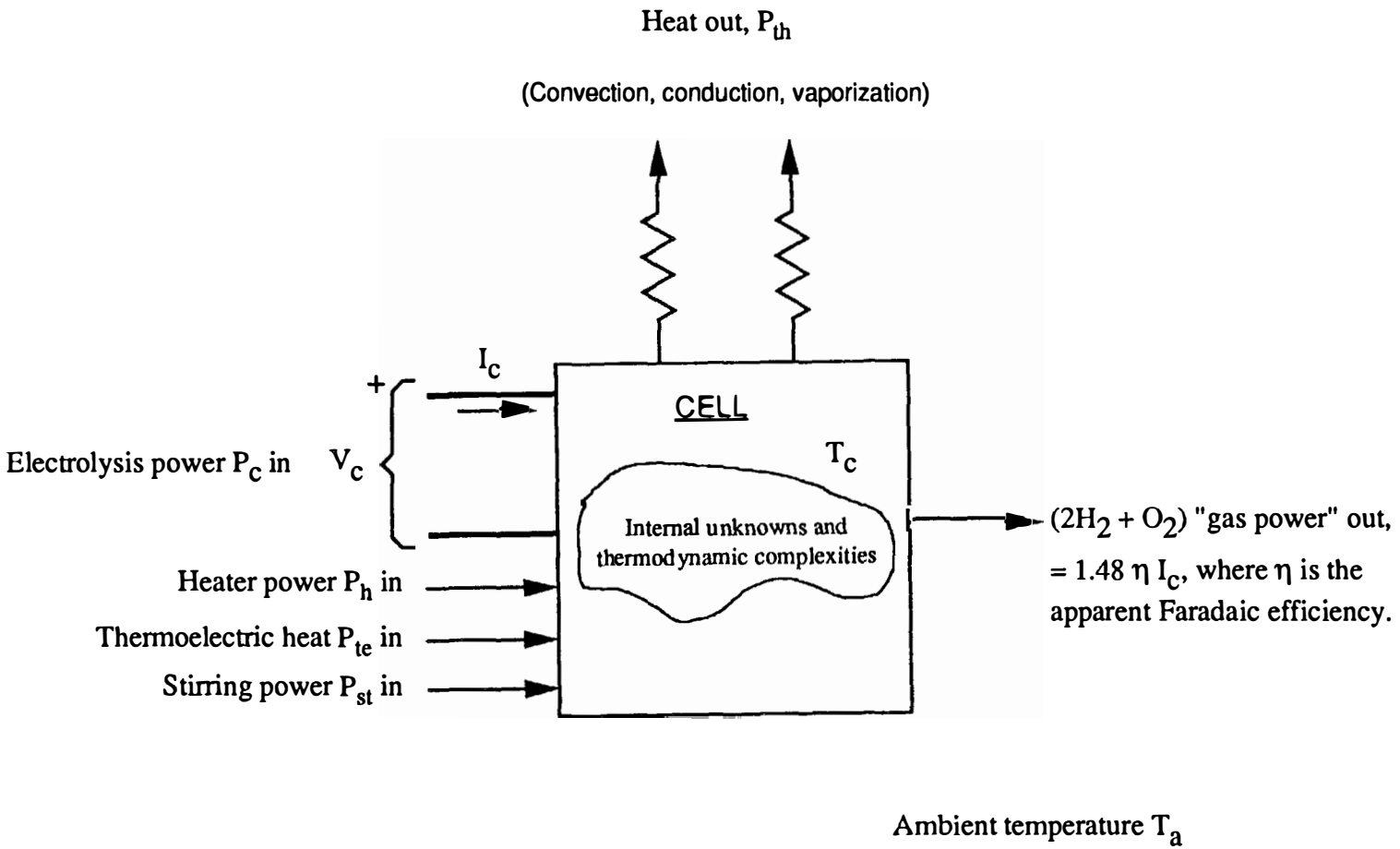

Figure 3. Identification of the cell input and output powers considered in the analysis of excess heat.

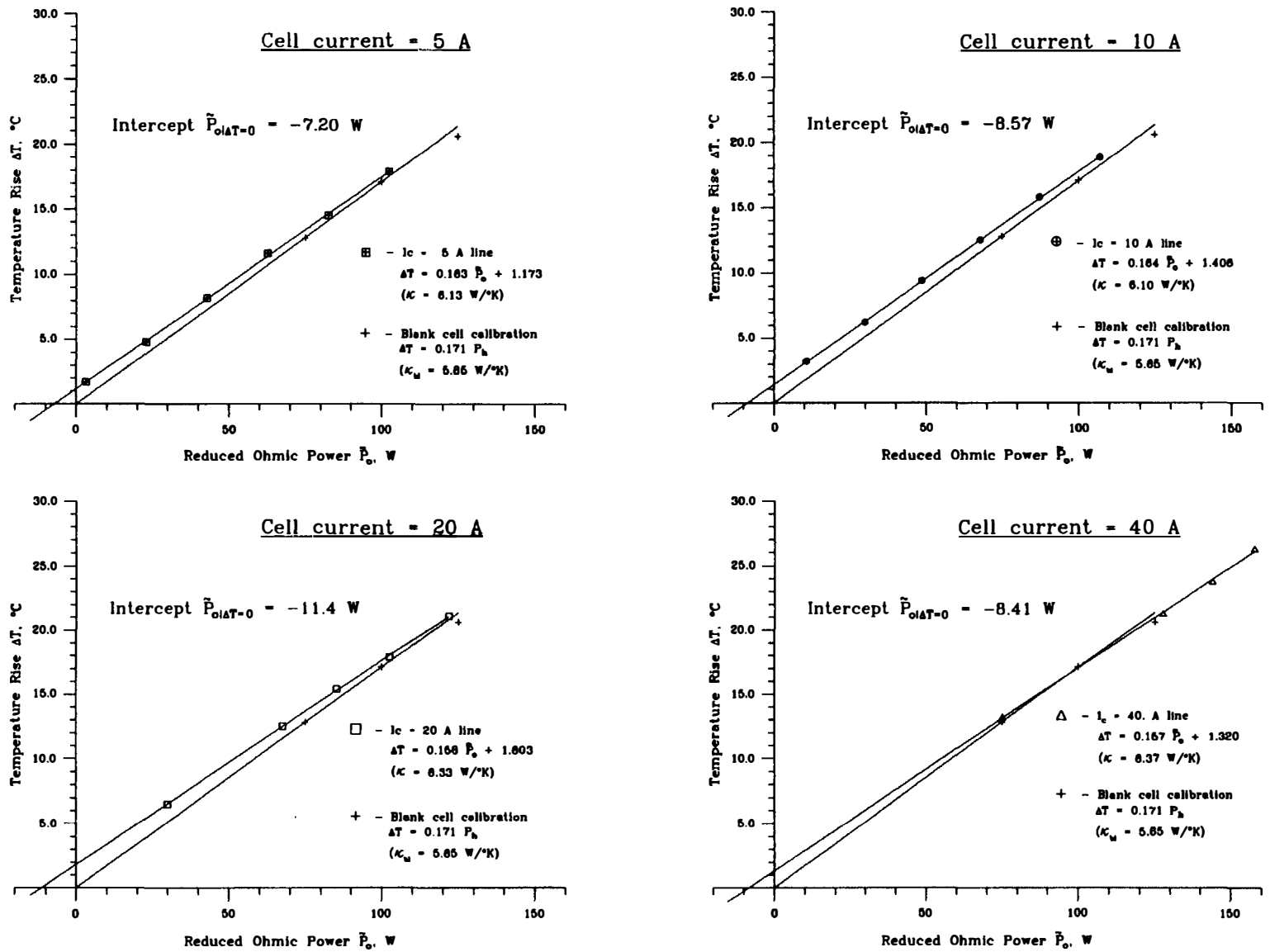

Figure 4. On–the–fly thermal calibration of the active cell for 4 selected dc electrolysis currents. The apparent excess heat is the negative intercept $-\tilde{P}_{o|\Delta T=0}$ of the fitted line with the $\tilde{P}_o$–axis. The blank cell calibration line is repeated in each plot for comparison of thermal conduction.

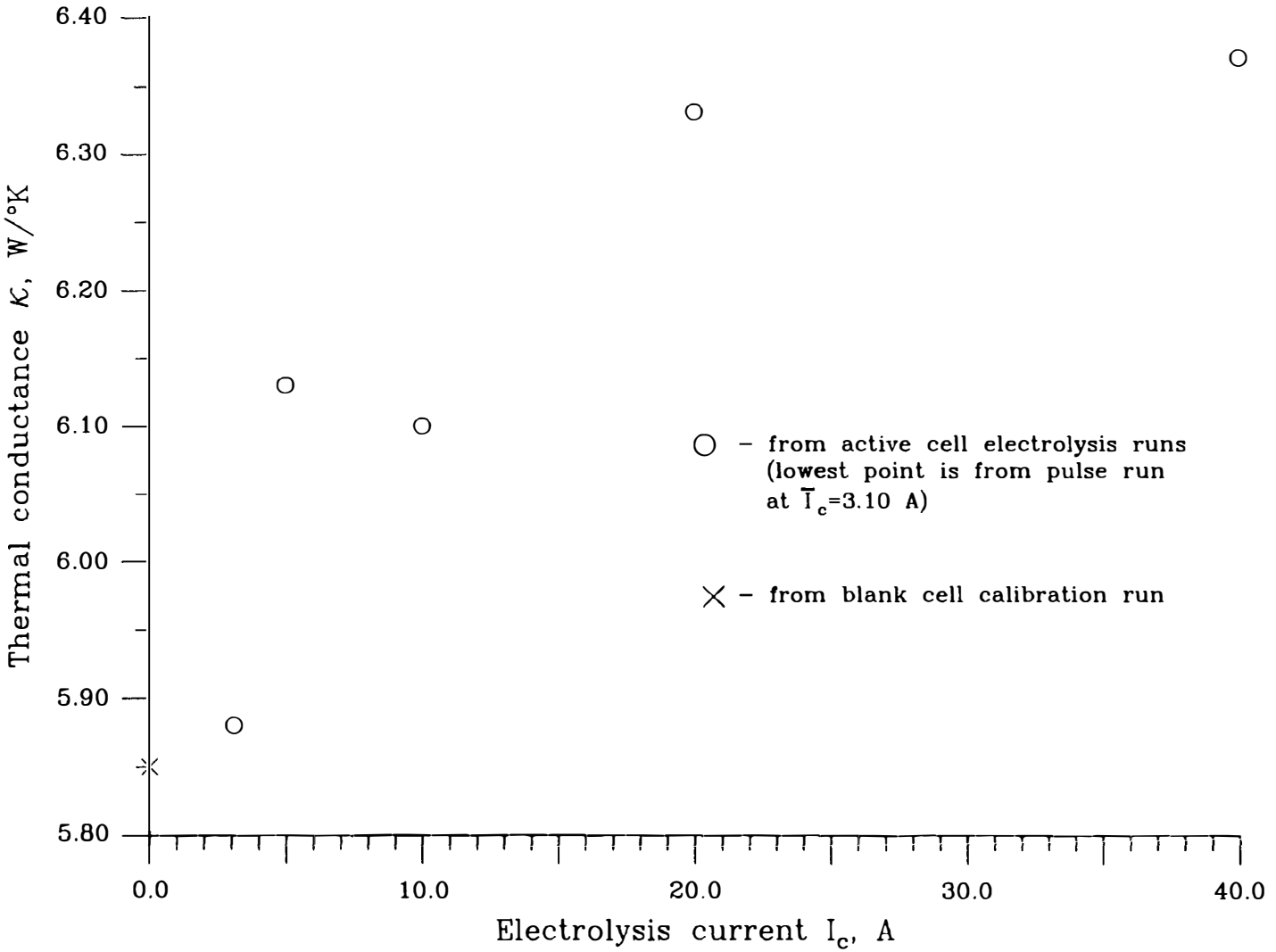

Figure 5. Scatter plot of cell thermal conductance K versus electrolysis current I_c, showing K for the blank cell and all active cell runs.

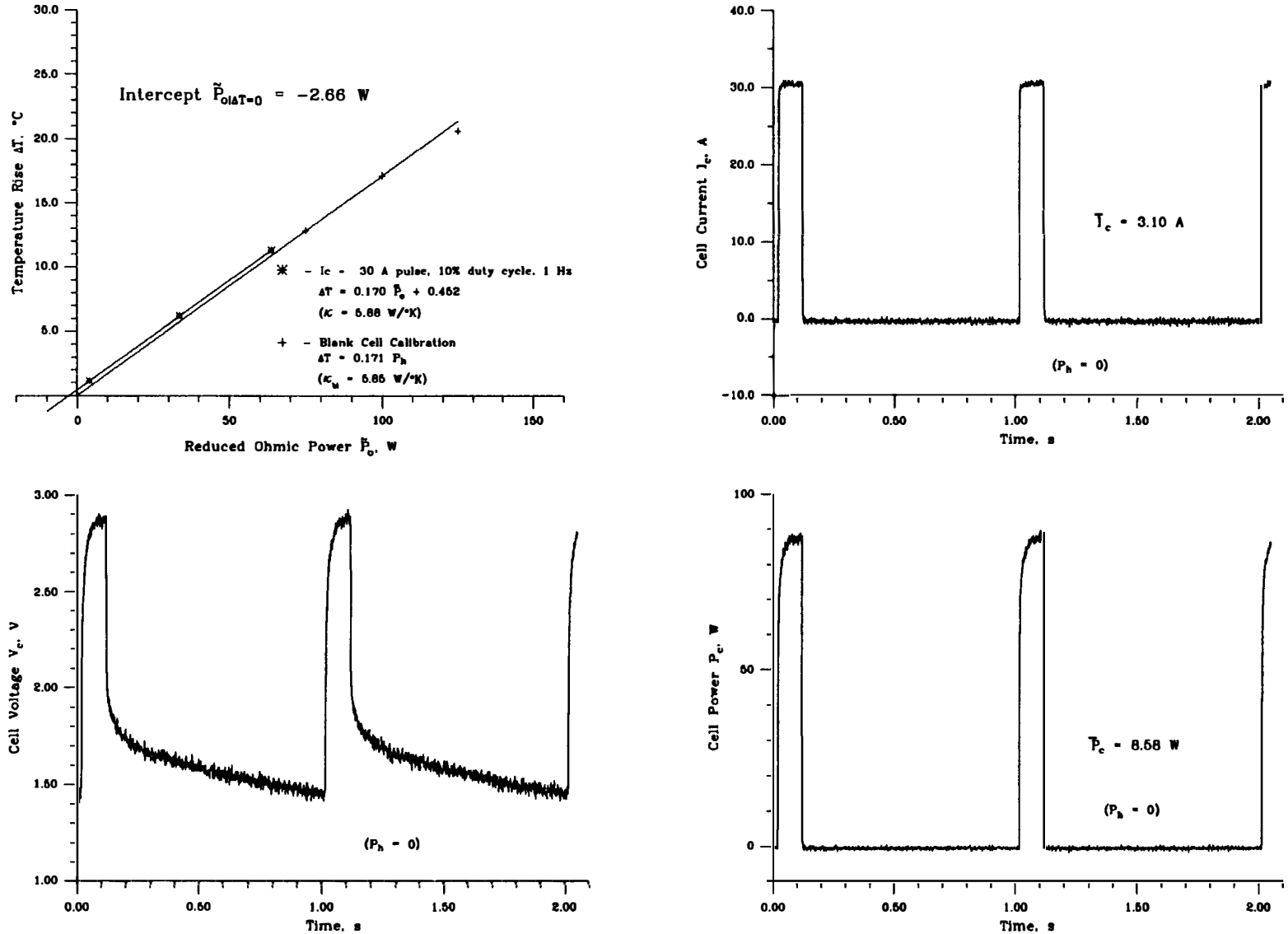

Figure 6. On−the−fly thermal calibration of the active cell for a pulsed electrolysis current. Waveforms of cell current, terminal voltage and power are shown at thermal equilibrium for zero heater power. Note near equality of active and blank cell thermal conductances.

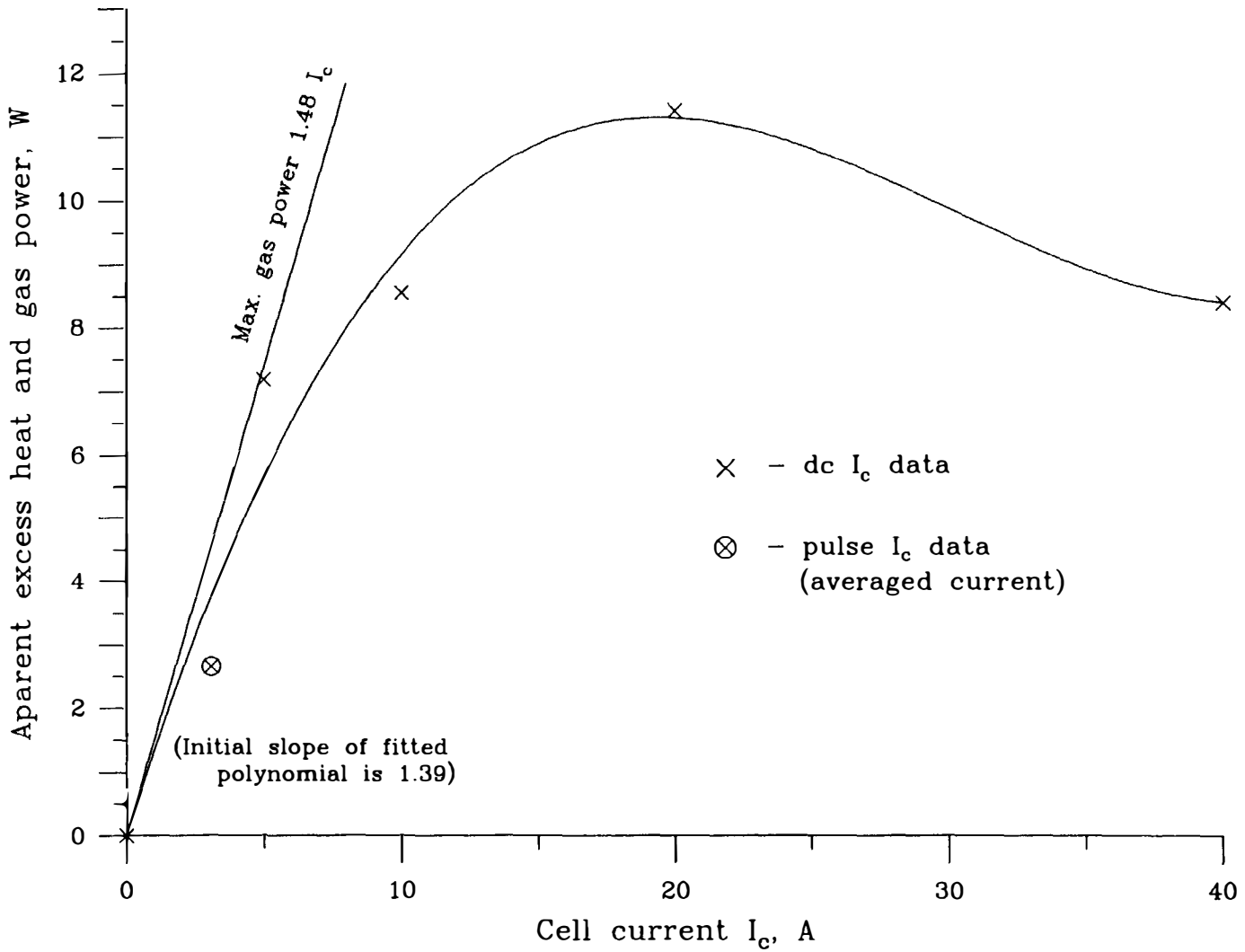

Figure 7. Plot of apparent excess power ($-\tilde{P}_{o|\Delta T=0}$) versus cell current I_c for all electrolysis runs. The fitted curve is a cubic polynomial through the origin, but has no special significance. The maximum gas power line is shown for comparison.

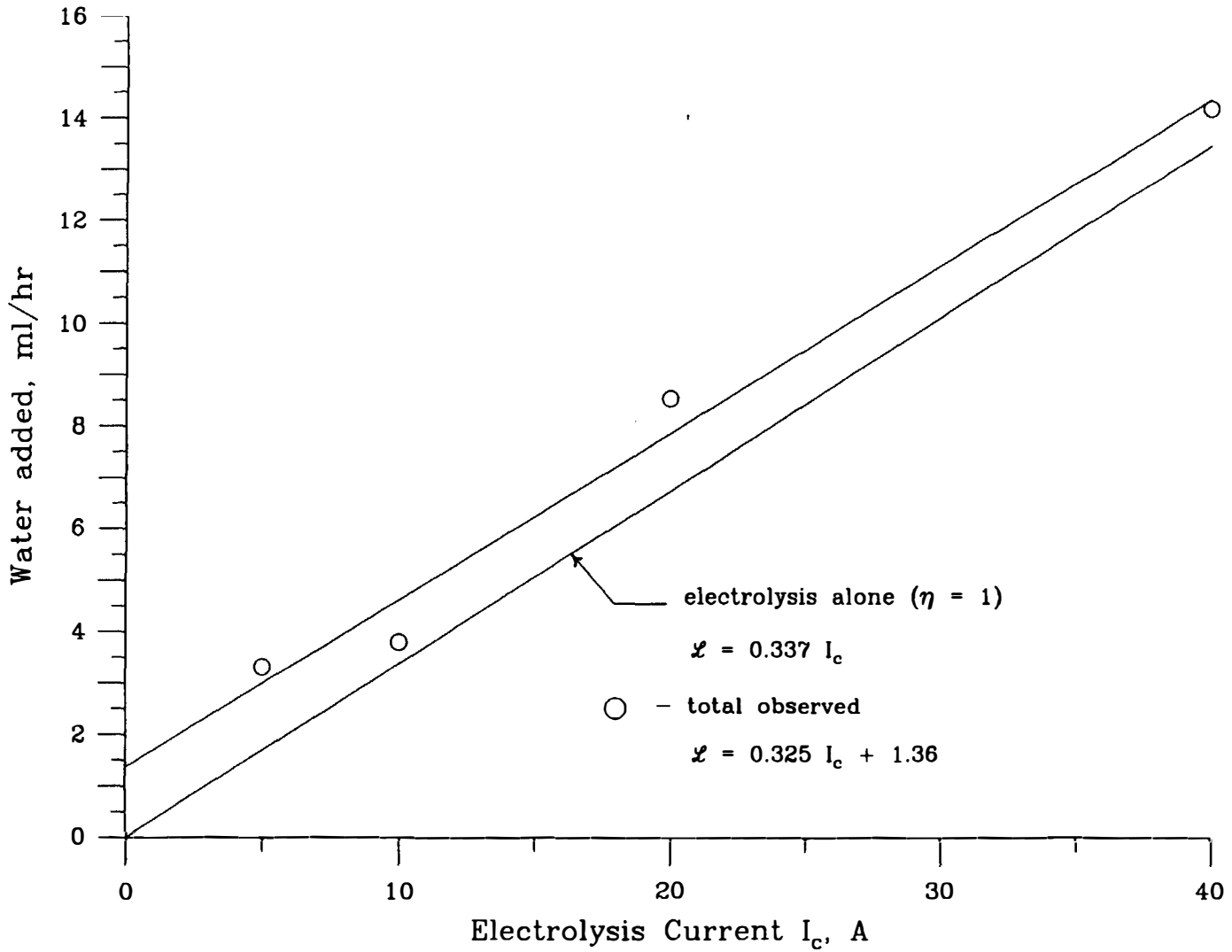

Figure 8. Comparison of the total observed and calculated electrolysis (η=1) alone water losses from the active cell at the four selected cell currents I_c. At each I_c, the losses have been averaged over the selected heater powers.

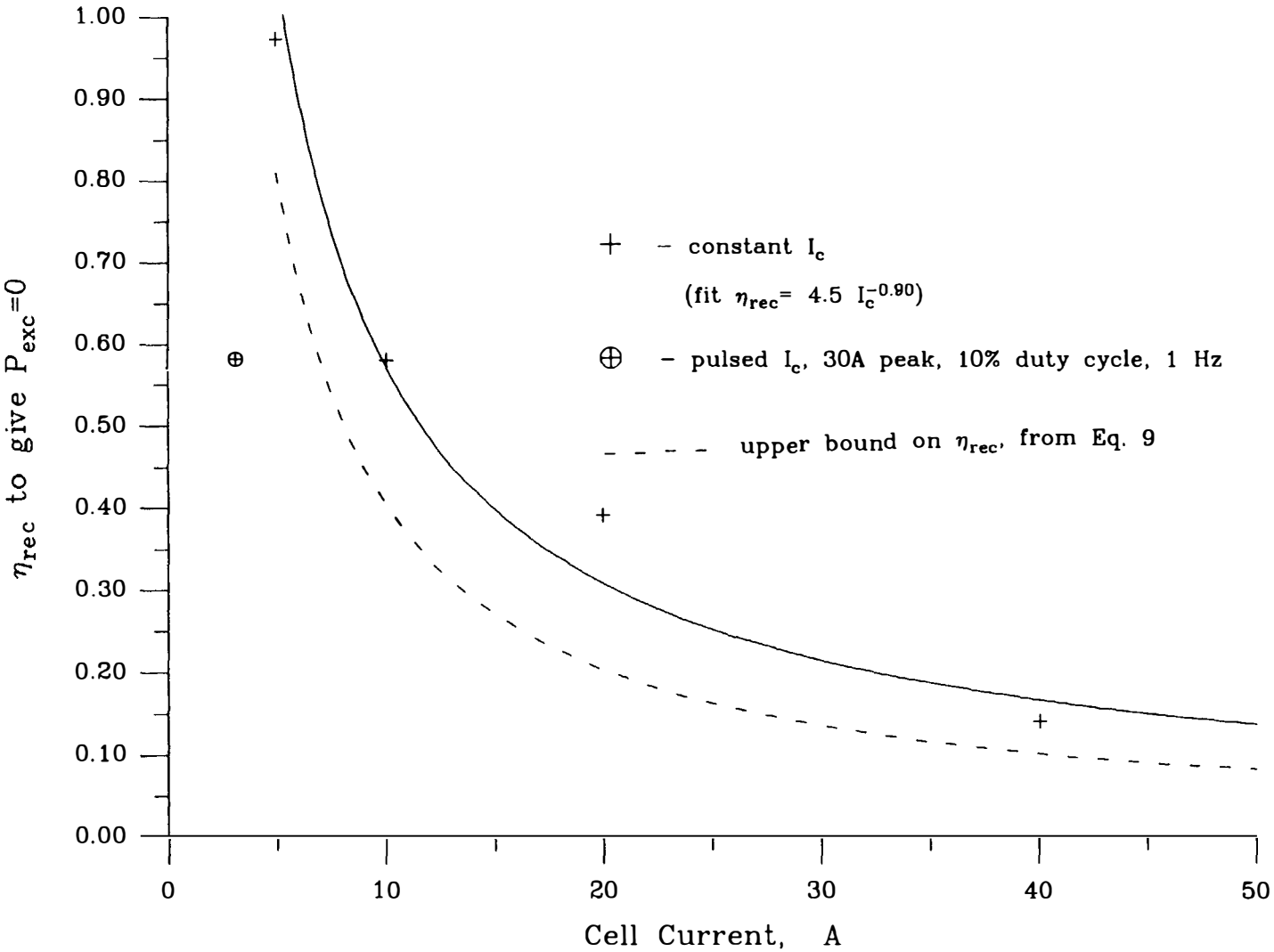

Figure 9. Oxygen–hydrogen recombination efficiency needed to account for all of the apparent excess heat at each of the experimental runs. Dashed curve shows the upper bound on η_{rec} imposed by Eq. 9 and experimental data of Fig. 8.

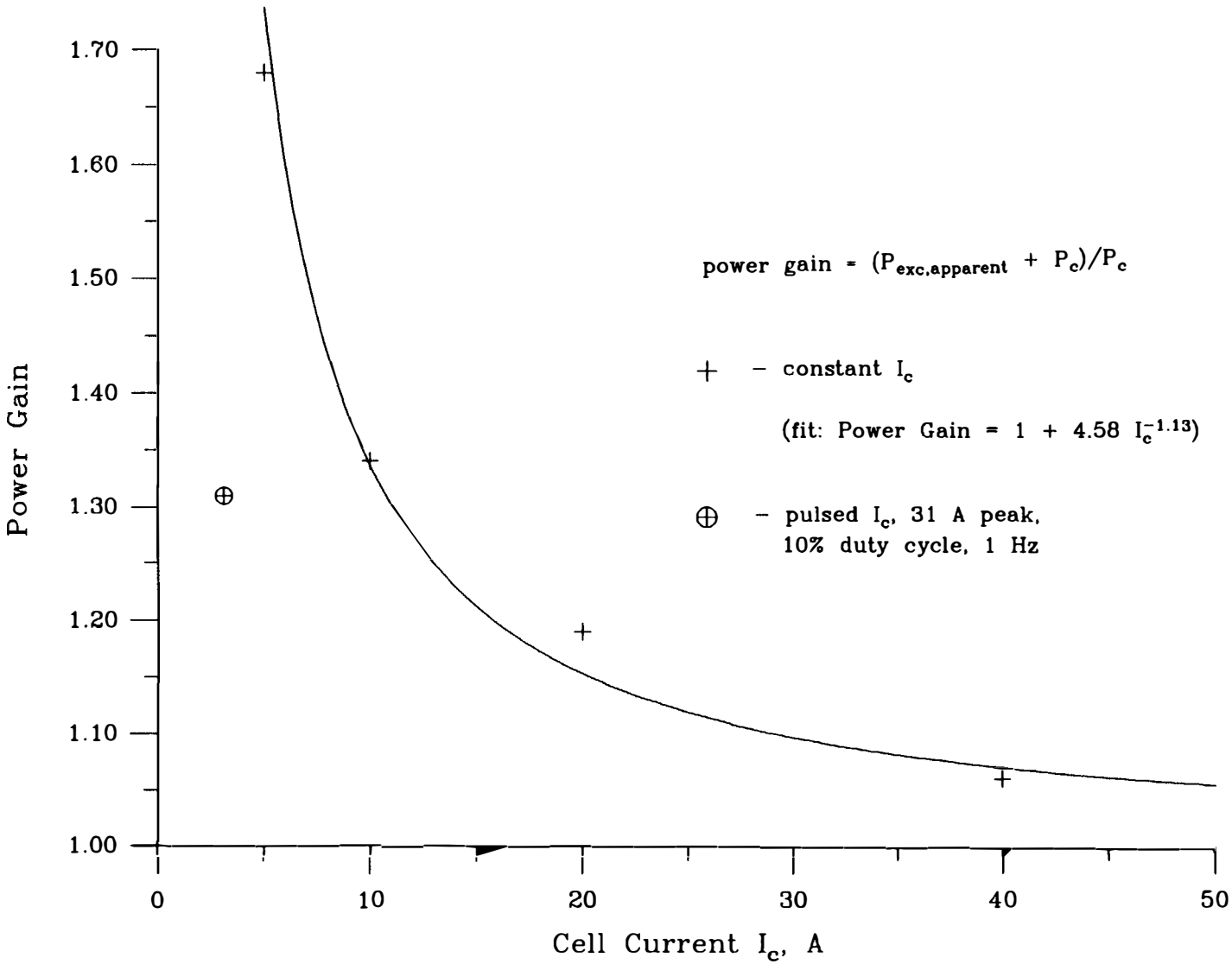

Figure 10. Power gain based on the apparent excess power observed at the selected cell currents I_c. All chemically stored energy is considered as part of the output.

REPORT DOCUMENTATION PAGE

Form Approved
OMB No. 0704-0188

1. AGENCY USE ONLY (*Leave blank*)	2. REPORT DATE	3. REPORT TYPE AND DATES COVERED
	February 1996	Technical Memorandum

4. TITLE AND SUBTITLE

Replication of the Apparent Excess Heat Effect in a Light Water—Potassium Carbonate—Nickel Electrolytic Cell

5. FUNDING NUMBERS

WU-307-51-00

6. AUTHOR(S)

Janis M. Niedra, Ira T. Myers, Gustave C. Fralick, and Richard S. Baldwin

7. PERFORMING ORGANIZATION NAME(S) AND ADDRESS(ES)

National Aeronautics and Space Administration
Lewis Research Center
Cleveland, Ohio 44135-3191

8. PERFORMING ORGANIZATION REPORT NUMBER

E-10118

9. SPONSORING/MONITORING AGENCY NAME(S) AND ADDRESS(ES)

National Aeronautics and Space Administration
Washington, D.C. 20546-0001

10. SPONSORING/MONITORING AGENCY REPORT NUMBER

NASA TM-107167

11. SUPPLEMENTARY NOTES

Janis M. Niedra, NYMA, Inc., 2001 Aerospace Parkway, Brook Park, Ohio 44142 (work funded by NASA Contract NAS3-27186); Ira T. Myers, Gustave C. Fralick, and Richard S. Baldwin, NASA Lewis Research Center. Responsible person, Gustave C. Fralick, organization code 2510, (216) 433-3645.

12a. DISTRIBUTION/AVAILABILITY STATEMENT

Unclassified - Unlimited
Subject Categories 44 and 70

This publication is available from the NASA Center for Aerospace Information, (301) 621-0390.

12b. DISTRIBUTION CODE

13. ABSTRACT (*Maximum 200 words*)

Replication of experiments claiming to demonstrate excess heat production in light water-Ni-K_2CO_3 electrolytic cells was found to produce an apparent excess heat of 11 W maximum, for 60 W electrical power into the cell. Power gains range from 1.06 to 1.68. The cell was operated at four different dc current levels plus one pulsed current run at 1 Hz, 10% duty cycle. The 28 liter cell used in these verification tests was on loan from a private corporation whose own tests with similar cells are documented to produce 50 W steady excess heat for a continuous period exceeding hundreds of days. The apparent excess heat can not be readily explained either in terms of nonlinearity of the cell's thermal conductance at a low temperature differential or by thermoelectric heat pumping. However, the present data do admit efficient recombination of dissolved hydrogen-oxygen as an ordinary explanation. Calorimetry methods and heat balance calculations for the verification tests are described. Considering the large magnitude of benefit if this effect is found to be a genuine new energy source, a more thorough investigation of evolved heat in the nickel-hydrogen system in both electrolytic and gaseous loading cells remains warranted.

14. SUBJECT TERMS	15. NUMBER OF PAGES
Anomalous heat cell; Energy source; Electrolytic cell; Space power; Calorimetry; Cold fusion; Light water cell	22
	16. PRICE CODE: A03

17. SECURITY CLASSIFICATION OF REPORT	18. SECURITY CLASSIFICATION OF THIS PAGE	19. SECURITY CLASSIFICATION OF ABSTRACT	20. LIMITATION OF ABSTRACT
Unclassified	Unclassified	Unclassified	

National Aeronautics and
Space Administration

Lewis Research Center
21000 Brookpark Rd.
Cleveland, OH 44135-3191